
Incorporating Metabolic Information into LLMs for Anomaly Detection in Clinical Time-Series

Maxx Richard Rahman
Saarland University & DFKI
Germany
m.rahman@iss.uni-saarland.de

Ruoxuan Liu
DFKI
Germany
ruoxuan.liu@dfki.de

Wolfgang Maass
Saarland University & DFKI
Germany
wolfgang.maass@dfki.de

Abstract

Anomaly detection in clinical time-series holds significant potential in identifying suspicious patterns in different biological parameters. This paper proposes a targeted method that incorporates the clinical domain knowledge into LLMs to improve their ability to detect anomalies. The Metabolism Pathway-driven Prompting (MPP) approach is introduced, which integrates the information about metabolic pathways to better capture the structural and temporal changes in biological samples. We applied our method for doping detection in sports, focusing on steroid metabolism, and evaluated using real-world data from athletes. The results show that our method improves anomaly detection performance by leveraging metabolic context, providing an improved prediction of suspicious samples in athletes' profiles.

1 Introduction

Clinical time series, also known as longitudinal profiles of individuals, represent repeated measurements of biological samples such as blood, urine, or other biological specimens collected over time [1,2]. These profiles are important in capturing the dynamic nature of biological processes, as they provide a time-evolving perspective of various physiological processes. The biomarkers measured within these samples often reflect underlying metabolic pathways [3].

In clinical settings, anomaly detection in these longitudinal profiles is an important task [4]. Identifying abnormal behaviour in such data can reveal critical insights, ranging from disease diagnosis to sample tampering as potential doping activity in sports [5,6]. It mainly helps biochemists or clinicians to monitor biological and physiological changes over time and detect suspicious behaviour. Therefore, anomaly detection plays a significant role in both sports integrity and healthcare. Several studies have highlighted the potential and limitations of Large Language Models (LLMs) in clinical domain-specific tasks [7,8,9]. Despite their success in text generation, completion tasks, etc., their ability to process and analyse clinical time-series data, particularly in the context of metabolic pathways and biological changes, remains under explored [10,11]. Understanding how these models can leverage metabolic information to make informed decisions is critical for improving their performance in anomaly detection tasks.

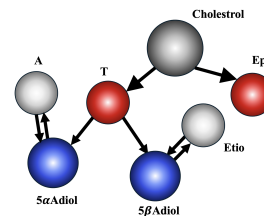


Figure 1: Simplified steroid pathway.

This paper aims to understand the current capabilities of LLMs in handling longitudinal data and leveraging domain-specific knowledge for anomaly detection tasks. Specifically, a targeted prompting method is proposed by integrating metabolic pathway structures into LLMs to improve their ability to detect anomalies based on the contextual understanding. We demonstrate the effectiveness of our approach in doping detection in sports, where it is applied to detect suspicious urine samples within athletes’ longitudinal profiles. These profiles include the concentrations of different metabolites, reflecting the steroid metabolism as shown in Fig.1, and are important for identifying potential doping activities [12,13]. The key contributions of our paper can be summarised as follows:

- Metabolism Pathway-driven Prompting (MPP) is proposed, incorporating information about metabolic pathway structure and the temporal evolution of different metabolites into LLMs for anomaly detection task.
- The effectiveness of this method is demonstrated in the context of doping detection in sports and compare it with the baseline prompting methods like zero-shot learning, in-context learning and chain-of-thought.

2 Proposed Method

2.1 Problem Formulation

Let the multivariate clinical time-series data be represented as longitudinal profile of athletes $X = \{x_1, x_2, \dots, x_n\}$, where $x_t \in \mathbb{R}^m$ represents the measurements at time t , containing total m metabolite and $x_{t,i}$ represents the measurement of metabolite i at time t . The temporal difference is defined as $\Delta x_{t,i}^T = x_{t,i} - x_{(t-1),i}$ representing the change in metabolite i over time. The anomaly detection task is to learn a function $f(x_t)$ that gives an anomaly score to each sample x_t in the longitudinal profile X . The function flags the anomalous sample if the magnitude of the sum of $\Delta x_{t,i}^T$ exceeds a predefined threshold δ , indicating significant deviation from the expected change:

$$f(x_t) = \begin{cases} 1, & \text{if } \left| \sum_{i=1}^m \Delta x_{t,i}^T \right| > \delta, \\ 0, & \text{otherwise.} \end{cases} \quad (1)$$

The metabolic structural difference is defined as $\Delta x_{t,i}^M = x_{t,i} - x_{t,(i+1)}$ which needs to be considered.

2.2 Metabolism Pathway-driven Prompting (MPP)

A targeted prompting method is proposed, integrating metabolic pathway structures and their temporal evolution as shown in Fig.2. First, LLM (**Pre-Prompt I**) is tasked to analyse the longitudinal profile and detect anomalies using zero-shot learning. Here, the LLM usually considers the temporal changes between consecutive samples. If these changes exceed the statistically significant threshold, it flags the corresponding sample as anomalous with an explanation. In a different session, we input LLM (**Pre-Prompt II**) with temporal and metabolic graph representation of the given longitudinal profile and task to extract the domain-specific contextual information from these graph structures. The LLM generates a detailed textual explanation by assessing whether the temporal changes are consistent with the expected metabolic behaviour based on known pathways. Next, the textual representation of domain knowledge is provided to the previous LLM, which is then tasked to rethink (**Prompt**) by incorporating this domain-specific information. The LLM refines the initial prediction by combining the domain-specific information and provide more accurate, and contextually aware prediction.

Temporal Graph The graph $G_T = (V_T, E_T)$ represents the change in concentration levels of different steroids over time. Nodes are defined as $V_T = \{x_1, x_2, \dots, x_n\}$, where each node x_t corresponds to the sample in the longitudinal profile and the node feature represents the measurements for the m steroids. The edges $E_T = \{w_T(x_1 \rightarrow x_2), w_T(x_2 \rightarrow x_3), \dots, w_T(x_{n-1} \rightarrow x_n)\}$ represent transitions between nodes over time, connecting the samples between successive time points and the edge weights as the Euclidean distance between the steroid levels at two time points and normalized to the range $[0, 1]$, incorporating the changes in all m steroids. For the edge connecting x_{n-1} and x_n , the weight could be calculated as:

$$w_T(x_{n-1} \rightarrow x_n) = \sqrt{\sum_{i=1}^m (x_{n-1,i} - x_{n,i})^2} \quad (2)$$

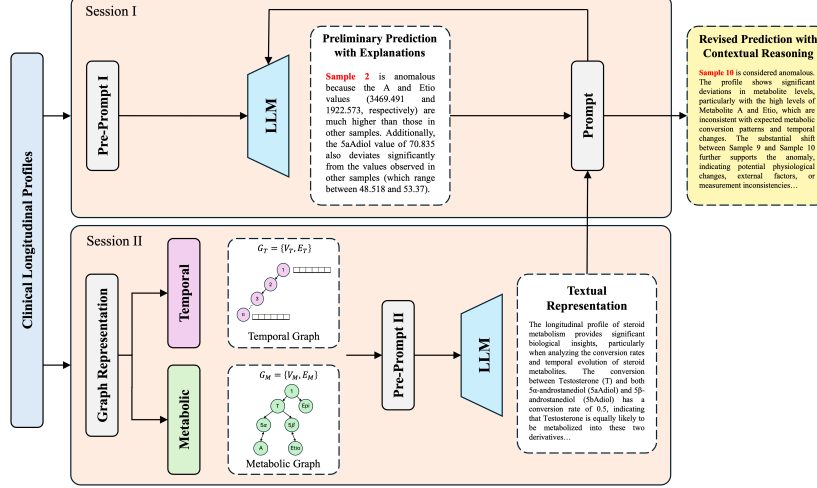


Figure 2: Schematic diagram of Metabolism Pathway-driven Prompting (MPP) method.

Metabolic Graph The graph $G_M = (V_M, E_M)$ represents the directional flow of m different metabolites (in this case steroids) in the pathway. Nodes are defined as $V_M = \{S_1, S_2, \dots, S_m\}$, where each node S_i represents a steroid. The edges E_M represent the interactions or metabolic conversions between these steroids. The weight of an edge $w_M(S_i \rightarrow S_j)$ represents the conversion rate from steroid S_i to steroid S_j , where $i, j = 1, 2, \dots, m$ and $i \neq j$. If there is no conversion between two steroids, the corresponding entry is zero.

$$E_M = \begin{pmatrix} 0 & w_M(S_1 \rightarrow S_2) & w_M(S_1 \rightarrow S_3) & \dots & w_M(S_1 \rightarrow S_m) \\ w_M(S_2 \rightarrow S_1) & 0 & w_M(S_2 \rightarrow S_3) & \dots & w_M(S_2 \rightarrow S_m) \\ w_M(S_3 \rightarrow S_1) & w_M(S_3 \rightarrow S_2) & 0 & \dots & w_M(S_3 \rightarrow S_m) \\ \vdots & \vdots & \vdots & \ddots & \vdots \\ w_M(S_m \rightarrow S_1) & w_M(S_m \rightarrow S_2) & w_M(S_m \rightarrow S_3) & \dots & 0 \end{pmatrix} \quad (3)$$

3 Experiments

Datasets Two real-world datasets (**Steroid-M** and **Steroid-F**) were used, consisting of longitudinal steroid profiles collected from male and female athletes, respectively [14,15]. The Steroid-M dataset contains 755 profiles with 4214 samples and Steroid-F dataset contains 375 profiles with 2307 samples. The data contains less than 20% anomalous longitudinal profile.

Models and Metrics Experiments are conducted using different open-source LLMs: (i) LLaMa 2-7B [16], (ii) Mistral-7B [17], (iii) Falcon-7B [18], and (iv) GPT2 [19]. These models are selected due to their efficiency in providing quicker results, which is particularly suitable for the size of the dataset. The performance of the proposed method is compared with various baseline prompting methods, including Zero-Shot prompting (ZS) [20], In-Context Learning (ICL) [21], and Chain-of-Thought (CoT) [22], as well as two non-LLM-based models, IsoForest [23] and β -VAE [24]. Classification metrics such as accuracy, sensitivity, specificity, and F1-score are used for the anomaly detection task.

4 Results

Performance Comparison Table 1 shows that by incorporating domain-specific knowledge of metabolic pathways, MPP improves the LLMs' understanding of clinical data, leading to better performance. For the LLaMA 2-7B model, MPP achieves an accuracy of 71.4% and an F1 score of 57.0%, outperforming ZS's 65.2% accuracy and 40.3% F1 score on Steroid-M. Notably, MPP improves both sensitivity and specificity, which is important in clinical settings to balance correctly identifying actual anomalies while minimising false positives. In contrast, ICL and CoT generally underperform due to their lack of domain-specific guidance, i.e., ICL with GPT2 on Steroid-M

Table 1: Performance comparison of our proposed method with different baseline methods.

Model	Method	Steroid-M				Steroid-F			
		Acc.	Sens.	Spec.	F1	Acc.	Sens.	Spec.	F1
LLaMA 2-7B	ZS	0.652	0.912	0.563	0.403	0.402	0.567	0.382	0.250
	ICL	0.563	0.012	0.710	0.005	0.458	0.008	0.506	0.002
	CoT	0.228	0.526	0.130	0.208	0.426	0.506	0.381	0.250
	MPP	0.714	0.966	0.630	0.570	0.634	0.922	0.464	0.592
Mistral-7B	ZS	0.763	0.931	0.632	0.578	0.724	0.012	0.905	0.028
	ICL	0.834	0.920	0.753	0.677	0.506	0.026	0.636	0.009
	CoT	0.501	0.894	0.598	0.517	0.626	0.012	0.752	0.002
	MPP	0.895	0.928	0.882	0.808	0.758	0.356	0.893	0.198
Falcon-7B	ZS	0.352	0.960	0.125	0.364	0.395	0.308	0.474	0.406
	ICL	0.560	0.014	0.710	0.005	0.527	0.472	0.536	0.338
	CoT	0.524	0.673	0.432	0.440	0.388	0.024	0.383	0.008
	MPP	0.767	0.950	0.632	0.578	0.684	0.820	0.522	0.605
GPT2	ZS	0.326	0.456	0.282	0.202	0.201	0.284	0.191	0.125
	ICL	0.282	0.006	0.355	0.002	0.229	0.004	0.253	0.001
	CoT	0.114	0.263	0.065	0.104	0.213	0.253	0.190	0.125
	MPP	0.357	0.483	0.315	0.285	0.317	0.461	0.232	0.296
Non-LLM	IsoForest	0.786	0.296	0.985	0.451	0.719	0.364	0.986	0.528
	β -VAE	0.752	0.006	0.992	0.012	0.681	0.002	0.994	0.004

yields only 28.2% accuracy and a negligible 0.2% F1 score. This underperformance highlights the importance of incorporating domain knowledge, as MPP does, to improve model performance for specialised tasks like clinical anomaly detection.

t-SNE Representation of Embeddings Fig.3 shows the cluster formation in the embedding space of the LLM output which represents the distinct latent patterns captured by each prompting method. Across all models, the MPP forms well-defined clusters, indicating that it consistently produces more structured and distinct embeddings compared to the other prompting methods. This suggests that MPP effectively captures relevant patterns for anomaly detection in clinical data, outperforming the more dispersed clustering seen in ZS and ICL. Notably, CoT also produces structured clusters, but MPP shows greater distinction and compactness, especially in LLaMA 2-7B and Mistral-7B, highlighting the efficacy of pathway-driven prompting.

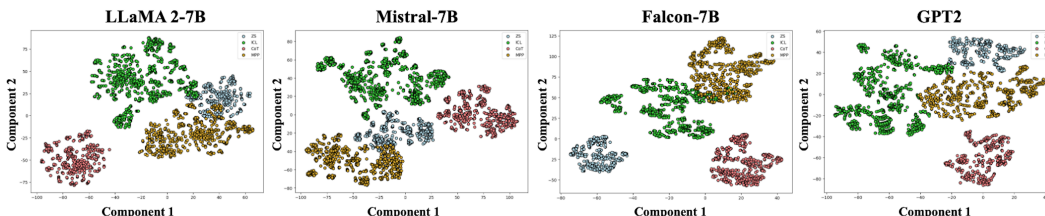


Figure 3: t-SNE representation of embeddings of the output from different prompting methods.

5 Conclusion

The Metabolism Pathway-driven Prompting (MPP) method is proposed to improve the anomaly detection within longitudinal data. By integrating the metabolic and temporal graphs for contextual understanding, MPP improves LLM’s ability to detect anomalies, particularly in steroid metabolism, which is important for doping detection in sports. The results show improved accuracy and sensitivity compared to conventional prompting methods, demonstrating the significance of incorporating domain-specific knowledge for more precise and effective anomaly detection in clinical applications.

References

- [1] Schüssler-Fiorenza Rose, S. M., Contrepois, K., Moneghetti, K. J., Zhou, W., Mishra, T., Mataraso, S., Snyder, M. P. (2019). A longitudinal big data approach for precision health. *Nature medicine*, 25(5), 792-804.
- [2] Albert, P. S. (1999). Longitudinal data analysis (repeated measures) in clinical trials. *Statistics in medicine*, 18(13), 1707-1732.
- [3] Monteiro, M. S., Carvalho, M., Bastos, M. L., Guedes de Pinho, P. (2013). Metabolomics analysis for biomarker discovery: advances and challenges. *Current medicinal chemistry*, 20(2), 257-271.
- [4] Huang, Z., Lu, X., Duan, H. (2012). Anomaly detection in clinical processes. *AMIA ... Annual Symposium proceedings. AMIA Symposium, 2012*, 370-379.
- [5] Moston, S., Engelberg, T. (2016). *Detecting doping in sport*. Routledge.
- [6] Kumar, Y., Koul, A., Singla, R., Ijaz, M. F. (2023). Artificial intelligence in disease diagnosis: a systematic literature review, synthesizing framework and future research agenda. *Journal of ambient intelligence and humanized computing*, 14(7), 8459-8486.
- [7] Karabacak, M., Margetis, K. (2023). Embracing large language models for medical applications: opportunities and challenges. *Cureus*, 15(5).
- [8] Nazi, Z. A., Peng, W. (2024, August). Large language models in healthcare and medical domain: A review. In *Informatics* (Vol. 11, No. 3, p. 57). MDPI.
- [9] Neveditsin, N., Lingras, P., Mago, V. (2024). Clinical Insights: A Comprehensive Review of Language Models in Medicine. *arXiv preprint arXiv:2408.11735*.
- [10] Helmy, M., Smith, D., Selvarajoo, K. (2020). Systems biology approaches integrated with artificial intelligence for optimized metabolic engineering. *Metabolic engineering communications*, 11, e00149.
- [11] Hager, P., Jungmann, F., Bhagat, K., Hubrecht, I., Knauer, M., Vielhauer, J., Rueckert, D. (2024). Evaluating and Mitigating Limitations of Large Language Models in Clinical Decision Making. *medRxiv*, 2024-01.
- [12] Piper, T., Geyer, H., Haenelt, N., Huelsemann, F., Schaenzer, W., Thevis, M. 2021. Current Insights into the Steroidal Module of the Athlete Biological Passport. *International Journal of Sports and Medicine* (42).
- [13] Rahman, M. R., Hussain, M., Piper, T., Geyer, H., Equey, T., Baume, N., Aikin, R., Maass, W. (2023). Modelling Metabolism Pathways using Graph Representation Learning for Fraud Detection in Sports. In *2023 IEEE International Conference on Digital Health (ICDH)* (pp. 158-168).
- [14] Rahman, M.R., Piper, T., Geyer, H., Equey, T., Baume, N., Aikin, R., Maass, W. 2022. Data Analytics for Uncovering Fraudulent Behaviour in Elite Sports. In *Proceedings of the 43rd International Conference on Information Systems (ICIS 2022)*.
- [15] Rahman, M.R., Khaliq, L.A., Piper, T., Geyer, H., Equey, T., Baume, N., Aikin, R., Maass, W. (2024). SACNN: Self Attention-based Convolutional Neural Network for Fraudulent Behaviour Detection in Sports. In *Proceedings of the International Joint Conference on Artificial Intelligence (IJCAI 24)*.
- [16] Touvron, H., Martin, L., Stone, K., Albert, P., Almahairi, A., Babaei, Y., Scialom, T. (2023). Llama 2: Open foundation and fine-tuned chat models. *arXiv preprint arXiv:2307.09288*.
- [17] Jiang, A. Q., Sablayrolles, A., Mensch, A., Bamford, C., Chaplot, D. S., Casas, D., Sayed, W. E. (2023). Mistral 7B. *arXiv preprint arXiv:2310.06825*.
- [18] Almazrouei, E., Alobeidli, H., Alshamsi, A., Cappelli, A., Cojocaru, R., Debbah, M., Penedo, G. (2023). The falcon series of open language models. *arXiv preprint arXiv:2311.16867*.
- [19] Radford, A., Wu, J., Child, R., Luan, D., Amodei, D., Sutskever, I. (2019). Language Models are Unsupervised Multitask Learners. *OpenAI Blog* (2019).
- [20] Li, Y. (2023). A practical survey on zero-shot prompt design for in-context learning. *arXiv:2309.13205*.
- [21] Yao, B., Chen, G., Zou, R., Lu, Y., Li, J., Zhang, S., Wang, D. (2024). More Samples or More Prompts? Exploring Effective Few-Shot In-Context Learning for LLMs with In-Context Sampling. In *Findings of the Association for Computational Linguistics: NAACL 2024* (pp. 1772-1790).
- [22] Cohn, C., Hutchins, N., Le, T., Biswas, G. (2024). A chain-of-thought prompting approach with llms for evaluating students' formative assessment responses in science. In *Proceedings of the AAAI Conference on Artificial Intelligence* (Vol. 38, No. 21, pp. 23182-23190).
- [23] Liu, F.T., Ting, K.M., and Zhou, Z.-H. (2008). Isolation-based anomaly detection. In *2008 Eighth IEEE International Conference on Data Mining*, pages 413-422. IEEE, 2008.

[24] Higgins, I., Matthey, L., Pal, A., Burgess, C., Glorot, X., Botvinick, M., Mohamed, S., and Lerchner, A. (2017). beta-VAE: Learning basic visual concepts with a constrained variational framework. In International Conference on Learning Representations, 2017.

A Prompting Methods

A.1 Zero-Shot Learning

It involves making predictions or identifying anomalies without explicit task-specific training. For longitudinal clinical data, we task LLM to infer whether certain samples are anomalous based on its prior general knowledge about statistical significance and typical clinical trends. Let $X = \{x_1, x_2, \dots, x_n\}$, where $x_t \in \mathbb{R}^m$ represents the measurements at time t and let A_t represent an anomaly indicator, where:

$$A_t = \begin{cases} 1, & \text{if an anomaly is detected at time } t, \\ 0, & \text{otherwise.} \end{cases} \quad (4)$$

The model attempts to predict A_t directly from the input data X without prior training on labeled clinical anomaly data. Fig.4 shows a prompt that we used for an example longitudinal profile.

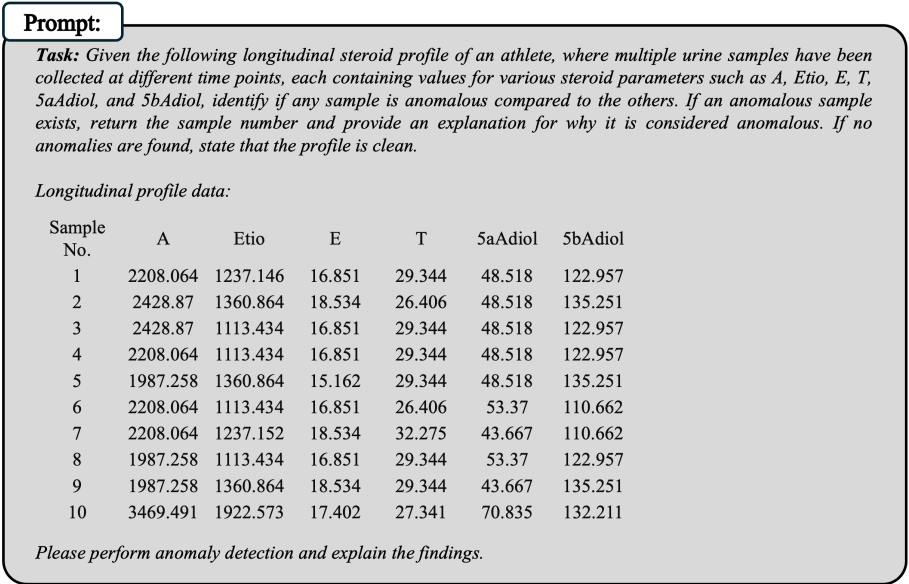


Figure 4: Example Prompt for Zero-shot Learning.

A.2 In-Context Learning

It involves providing the model with a few examples of what constitutes "normal" and "anomalous" patterns within the context of the prompt. The LLM uses these examples to generalise and apply its learned knowledge to unseen data points in the clinical data. Let us consider we are provided with k examples of clinical longitudinal profiles over time, which are labeled $\{(X_1, A_1), (X_2, A_2), \dots, (X_k, A_k)\}$. These examples are included as part of the prompt.

Now, we give the longitudinal profile X to LLM to infer the anomaly label A_t by leveraging the information gained from the previous examples.

$$A_t = f(X \mid \{(X_1, A_1), (X_2, A_2), \dots, (X_k, A_k)\}), \quad (5)$$

where function $f(\cdot)$ generalises from the given examples. Fig.5 shows a prompt that we used for an example longitudinal profile.

A.3 Chain-of-Thought (CoT)

It encourages the model to reason through a multi-step process, explicitly following a logical progression before reaching its conclusion. For anomaly detection in longitudinal clinical data, this means that LLM is prompted to analyse how clinical values evolve over time and their relationships with other biomarkers before flagging an anomaly. We gave the following instructions:

Prompt:

Information: Given the following longitudinal steroid profile of an athlete, where multiple urine samples have been collected at different time points, each containing values for various steroid parameters such as A, Etio, E, T, 5aAdiol, and 5bAdiol, identify if any sample is anomalous compared to the others. If an anomalous sample exists, return the sample number and provide an explanation for why it is considered anomalous. If no anomalies are found, state that the profile is clean.

Example 1:

Sample No.	A	Etio	E	T	5aAdiol	5bAdiol
1	2208.064	1237.146	16.851	29.344	48.518	122.957
2	2428.87	1360.864	18.534	26.406	48.518	135.251
3	2428.87	1113.434	16.851	29.344	48.518	122.957
4	2208.064	1113.434	16.851	29.344	48.518	122.957
5	1987.258	1360.864	15.162	29.344	48.518	135.251
6	2208.064	1113.434	16.851	26.406	53.37	110.662
7	2208.064	1237.152	18.534	32.275	43.667	110.662

Analysis:

Sample 7 is anomalous because the 5aAdiol and 5bAdiol values (43.667 and 110.662, respectively) deviate significantly from the rest of the samples, which range between 48.518 and 53.37 for 5aAdiol and between 122.957 and 135.251 for 5bAdiol.

Example 2:

Sample No.	A	Etio	E	T	5aAdiol	5bAdiol
1	2428.87	1360.864	18.534	26.406	48.518	135.251
2	3469.491	1922.573	17.402	27.341	70.835	132.211
3	1987.258	1360.864	15.162	29.344	48.518	135.251
4	2208.064	1237.146	16.851	29.344	48.518	122.957

Analysis:

Sample 2 is anomalous because the A and Etio values (3469.491 and 1922.573, respectively) are much higher than those in other samples. Additionally, the 5aAdiol value of 70.835 also deviates significantly from the values observed in other samples (which range between 48.518 and 53.37).

Task: Please analyze the below dataset, identify any anomalous samples, and provide an explanation.

Sample No.	A	Etio	E	T	5aAdiol	5bAdiol
1	2208.064	1237.146	16.851	29.344	48.518	122.957
2	2428.87	1360.864	18.534	26.406	48.518	135.251
3	2428.87	1113.434	16.851	29.344	48.518	122.957
4	2208.064	1113.434	16.851	29.344	48.518	122.957
5	1987.258	1360.864	15.162	29.344	48.518	135.251
6	2208.064	1113.434	16.851	26.406	53.37	110.662
7	2208.064	1237.152	18.534	32.275	43.667	110.662
8	1987.258	1113.434	16.851	29.344	53.37	122.957
9	1987.258	1360.864	18.534	29.344	43.667	135.251
10	3469.491	1922.573	17.402	27.341	70.835	132.211

Figure 5: Example Prompt for In-context Learning.

- **Step 1: Analyse the range of each parameter** We task to examine the values of each steroid parameter across all the samples and calculate the mean (μ) and standard deviation (σ) for each parameter to quantify the "normal" range:

$$\mu = \frac{1}{n} \sum_{i=1}^n x_i \quad \text{and} \quad \sigma = \sqrt{\frac{1}{n} \sum_{i=1}^n (x_i - \mu)^2} \quad (6)$$

- **Step 2: Identify deviations across parameters** After understanding the range of each parameter, we focus on finding deviations across multiple parameters within a sample to check if a particular sample shows unusually high or low values for more than one parameter. In addition, ratios between key parameters such as the Testosterone-to-Epitestosterone (T/E) ratio—can be useful indicators of abnormalities. Similarly, other useful ratios include:

$$R_{T/E} = \frac{T}{E}, \quad R_{T/5\alpha \text{ Adiol}} = \frac{T}{5\alpha \text{ Adiol}}, \quad R_{T/5\beta \text{ Adiol}} = \frac{T}{5\beta \text{ Adiol}} \quad (7)$$

Sudden deviations in these ratios compared to the rest of the samples can signal an abnormal sample.

- **Step 3: Conclude the anomalous samples** Finally, based on the findings from previous steps, we identify and return the sample number(s) that show significant anomalies. The anomaly is flagged based on either exceeding the calculated range ($\mu \pm 2\sigma$) or abnormal changes in the parameter ratios. If no significant anomalies are detected, the conclusion should state that the profile is clean. Fig.6 shows a prompt that we used for an example longitudinal profile.

Prompt:

Task: Given the following longitudinal steroid profile of an athlete, where multiple urine samples have been collected at different time points, each containing values for various steroid parameters (A, Etio, E, T, 5aAdiol, and 5bAdiol), perform anomaly detection.

Longitudinal Profile Data:

Sample No.	A	Etio	E	T	5aAdiol	5bAdiol
1	2208.064	1237.146	16.851	29.344	48.518	122.957
2	2428.87	1360.864	18.534	26.406	48.518	135.251
3	2428.87	1113.434	16.851	29.344	48.518	122.957
4	2208.064	1113.434	16.851	29.344	48.518	122.957
5	1987.258	1360.864	15.162	29.344	48.518	135.251
6	2208.064	1113.434	16.851	26.406	53.37	110.662
7	2208.064	1237.152	18.534	32.275	43.667	110.662
8	1987.258	1113.434	16.851	29.344	53.37	122.957
9	1987.258	1360.864	18.534	29.344	43.667	135.251
10	3469.491	1922.573	17.402	27.341	70.835	132.211

Step 1: Analyze the Range of Each Parameter
For each steroid parameter (A, Etio, E, T, 5aAdiol, 5bAdiol), look at the values across all samples and establish a general range or trend. Identify which samples fall significantly outside this range.

Step 2: Identify Deviations Across Parameters
Look for unusual changes in values that deviate from the norm, focusing on samples where multiple parameters change dramatically in relation to the rest. Calculate relevant ratios like T/E or T/5aAdiol if needed to spot further anomalies.

Step 3: Conclude the Anomalous Samples
Identify and return the sample number(s) that show significant anomalies in the steroid profile, explaining the reason for the anomaly based on the patterns observed. If no anomalies are found, state that the profile is clean.

Figure 6: Example Prompt for Chain-of-Thought.

B Metabolism Pathway-driven Prompting

Fig.7 shows a Pre-prompt I for LLM that we used for an example longitudinal profile. Fig.8 shows a pre-prompt II that we used in another session for the same longitudinal profile. Finally, Fig.9 shows a Prompt that integrates the response of the Pre-prompt II that we used for the same longitudinal profile.

Pre-Prompt I:

Task: Given the following longitudinal steroid profile of an athlete, where multiple urine samples have been collected at different time points, each containing values for various steroid parameters such as A, Etio, E, T, 5aAdiol, and 5bAdiol, identify if any sample is anomalous compared to the others. If an anomalous sample exists, return the sample number and provide an explanation for why it is considered anomalous. If no anomalies are found, state that the profile is clean.

Longitudinal profile data:

Sample No.	A	Etio	E	T	5aAdiol	5bAdiol
1	2208.064	1237.146	16.851	29.344	48.518	122.957
2	2428.87	1360.864	18.534	26.406	48.518	135.251
3	2428.87	1113.434	16.851	29.344	48.518	122.957
4	2208.064	1113.434	16.851	29.344	48.518	122.957
5	1987.258	1360.864	15.162	29.344	48.518	135.251
6	2208.064	1113.434	16.851	26.406	53.37	110.662
7	2208.064	1237.152	18.534	32.275	43.667	110.662
8	1987.258	1113.434	16.851	29.344	53.37	122.957
9	1987.258	1360.864	18.534	29.344	43.667	135.251
10	3469.491	1922.573	17.402	27.341	70.835	132.211

Please perform anomaly detection and explain the findings.

Figure 7: Pre-Prompt I for Metabolism Pathway-driven Prompting.

Pre-Prompt II:

Information: Given the domain knowledge representing in form of spatial and temporal graph explaining the steroid metabolism and the temporal evolution of metabolites respectively. In the spatial graph, each node represents a steroid metabolite, and edge weights represent conversion rates between from one metabolite to another. In the temporal graph, each node represents a sample, and the edge weights represent the distances between the samples, showing how the steroid profiles change over time.

Task: Generate a textual representation of this domain knowledge for the given longitudinal profile by extracting the biological information. Do not explain the graph structure.

- Include the detailed insights from the edge weights of the spatial graph which represent the conversion rate between the two metabolites.
- Include the detailed insights from the node matrix of the temporal graph which represent the concentration level of different metabolites in every sample (node).
- Include the detailed insights from the edge weights of the temporal graph which represent the euclidean distance.

Spatial Graph

Node	1	A	Etio	Epi	T	5aAdiol	5bAdiol
1	0.0	0.0	0.0	0.5	0.5	0.0	0.0
A	0.0	0.0	0.0	0.0	0.0	0.0	0.0
Etio	0.0	0.0	0.0	0.0	0.0	0.0	0.0
Epi	0.0	0.0	0.0	0.0	0.0	0.0	0.0
T	0.0	0.0	0.0	0.0	0.0	0.5	0.5
5aAdiol	0.0	1.0	0.0	0.0	0.0	0.0	0.0
5bAdiol	0.0	0.0	1.0	0.0	0.0	0.0	0.0

Temporal Graph

Node	A	Etio	E	T	5aAdiol	5bAdiol
1	2208.064	1237.146	16.851	29.344	48.518	122.957
2	2428.87	1360.864	18.534	26.406	48.518	135.251
3	2428.87	1113.434	16.851	29.344	48.518	122.957
4	2208.064	1113.434	16.851	29.344	48.518	122.957
5	1987.258	1360.864	15.162	29.344	48.518	135.251
6	2208.064	1113.434	16.851	26.406	53.37	110.662
7	2208.064	1237.152	18.534	32.275	43.667	110.662
8	1987.258	1113.434	16.851	29.344	53.37	122.957
9	1987.258	1360.864	18.534	29.344	43.667	135.251
10	3469.491	1922.573	17.402	27.341	70.835	132.211

Node	1	2	3	4	5	6	7	8	9	10
1	0.0	0.088	0.0	0.0	0.0	0.0	0.0	0.0	0.0	0.0
2	0.088	0.0	0.084	0.0	0.0	0.0	0.0	0.0	0.0	0.0
3	0.0	0.084	0.0	0.066	0.0	0.0	0.0	0.0	0.0	0.0
4	0.0	0.0	0.066	0.0	0.142	0.0	0.0	0.0	0.0	0.0
5	0.0	0.0	0.0	0.142	0.0	0.142	0.0	0.0	0.0	0.0
6	0.0	0.0	0.0	0.0	0.142	0.0	0.0	0.0	0.0	0.0
7	0.0	0.0	0.0	0.0	0.0	0.0	0.0	0.088	0.0	0.0
8	0.0	0.0	0.0	0.0	0.0	0.0	0.088	0.0	0.084	0.0
9	0.0	0.0	0.0	0.0	0.0	0.0	0.0	0.084	0.0	1.0
10	0.0	0.0	0.0	0.0	0.0	0.0	0.0	0.0	1.0	0.0

Figure 8: Pre-Prompt II for Metabolism Pathway-driven Prompting.

Prompt:

Task: Below is the information about the domain knowledge of the spatial and temporal behaviour of the longitudinal steroid profile. Use this information and think again about the anomolous sample in the longitudinal profile. If an anomolous sample exists, return the sample number and provide an explanation for why it is considered anomolous. If no anomalies are found, state that the profile is clean. These insights provide a detailed biological understanding of the temporal changes and metabolic conversion pathways, offering clues about physiological states, potential anomalies, or patterns within the steroid profile over time.

Information:

The longitudinal profile of steroid metabolism provides significant biological insights, particularly when analyzing the conversion rates and temporal evolution of steroid metabolites.

Metabolism Pathway:

The spatial graph offers a detailed view of the steroid metabolism, focusing on how metabolites are interconverted. The edge weights between metabolites represent the conversion rates, reflecting the intensity or likelihood of one metabolite converting into another. For example:

- The conversion between Testosterone (T) and both 5 α -androstanediol (5aAdiol) and 5 β -androstanediol (5bAdiol) has a conversion rate of 0.5, indicating that Testosterone is equally likely to be metabolized into these two derivatives.
- A notable conversion occurs between 5aAdiol and metabolite A with a conversion rate of 1.0, suggesting a very high or complete conversion of 5aAdiol into metabolite A.
- Additionally, 5bAdiol shows a weaker connection to Etiocholanolone (Etio) with a conversion rate of 0.1, implying a less significant metabolic conversion between these metabolites.
- No direct conversions are observed between other metabolites like Etio, Epiandrosterone (Epi), or metabolite A, indicating that these might represent metabolic endpoints or have indirect interactions not captured by the direct edge weights.

Temporal Evolution:

The temporal graph shows the evolution of steroid profiles across various samples, with Euclidean distances between nodes representing changes in metabolite concentrations over time. Larger distances between nodes indicate more substantial changes in steroid profiles between samples:

- The smallest distances are seen between samples 2 and 3 (0.0845) and samples 3 and 4 (0.0661), indicating minimal changes in the steroid profiles across these time points, reflecting stable or slightly fluctuating metabolism.
- In contrast, a significant change is observed between samples 9 and 10, with a distance of 1.0, pointing to a substantial shift in the steroid profile at this point in time, suggesting either a physiological response, external intervention, or an anomaly in metabolism.
- The temporal progression from sample 5 to 6 also shows a moderate shift with a distance of 0.1426, highlighting evolving metabolite levels.
- Metabolite A shows significant variation, starting at 2208.064 in sample 1 and rising to a peak of 3469.491 in sample 10. This indicates a substantial accumulation of metabolite A over time, suggesting it plays a key role in metabolic progression or reflects a stress response.
- Etio levels fluctuate as well, starting at 1237.146 in sample 1, dropping to 1113.434 across several samples, and rising to 1922.573 in sample 10, further indicating significant metabolic variation.
- 5aAdiol levels remain relatively stable, around 48.518 across most samples, except for sample 6 (53.37) and sample 10 (70.835), suggesting minor but important variations in 5 α -reduction activity.
- The concentration of Testosterone (T) exhibits some variation, particularly peaking at 32.275 in sample 7, but generally stabilizing around 29.344, implying consistent androgenic activity throughout most of the samples.

Figure 9: Prompt for Metabolism Pathway-driven Prompting.